Efficient Capture of CO2 from Simulated Flue Gas by Formation of TBAB or TBAF Semiclathrate Hydrates

ARTICLE *in* ENERGY & FUELS · AUGUST 2009

Impact Factor: 2.79 · DOI: 10.1021/ef9003329

5 AUTHORS, INCLUDING:

Shuanshi Fan
South China University of Technology
168 PUBLICATIONS **8,115** CITATIONS
SEE PROFILE

Shifeng Li
Shenyang University
21 PUBLICATIONS **289** CITATIONS
SEE PROFILE

Xuemei Lang
South China University of Technology
28 PUBLICATIONS **542** CITATIONS
SEE PROFILE

Yanhong Wang
Northeast Agricultural University
27 PUBLICATIONS **356** CITATIONS
SEE PROFILE

Efficient Capture of CO_2 from Simulated Flue Gas by Formation of TBAB or TBAF Semiclathrate Hydrates

Shuanshi Fan,*,† Shifeng Li,†,‡ Jingqu Wang,‡ Xuemei Lang,† and Yanhong Wang†

The Key Laboratory of Enhanced Heat Transfer and Energy Conversation, Ministry of Education, South China University of Technology, Guangzhou, 510640, China and School of Chemical Engineering, Dalian University of Technology, Dalian 116012, China

Received April 14, 2009. Revised Manuscript Received June 23, 2009

Capturing CO_2 by forming hydrate is an attractive technology for reducing the greenhouse effect. The most primary challenges are high energy consumption, low hydrate formation rate, and separation efficiency. This work presents efficient capture of CO_2 from simulated flue gas (CO_2 (16.60 mol %)/N_2 binary mixtures) by formation of semiclathrate hydrates at 4.5 and 7.1 °C and feed pressures ranging from 2.19 to 7.31 MPa. The effect of 0.293 mol % tetra-*n*-butyl ammonium bromide (TBAB) and tetra-*n*-butyl ammonium fluoride (TBAF) on the hydrate formation rate, reactor space velocity, and CO_2 separation efficiency was studied in a 1 L stirred reactor. The results showed the hydrate formation rate constant increased with increasing feed pressure and reached the maximum at 2.82×10^{-7} mol^2/(s·J) with TBAB and 8.26×10^{-7} mol^2/(s·J) with TBAF. The space velocity of the hydrate reactor increased with increasing feed pressure and reached a maximum of 13.46 h^{-1} with TBAB and 25.96 h^{-1} with TBAF. CO_2 recovery was about 50%, and the optimum CO_2 separation factor with TBAF was 36.98, which was about 4 times higher than that with TBAB in the range of feed pressure. CO_2 could be enriched to 90.40 mol % from simulated flue gas under low feed pressure by two stages of hydrate separation with TBAF. The results demonstrated that TBAB, especially TBAF, could accelerate hydrate formation. The space velocity of the hydrate reactor with TBAB or TBAF was higher than that with THF. CO_2 could be easily enriched in the hydrate phase by two stages of hydrate separation under gentle conditions.

1. Introduction

The emission of carbon dioxide (CO_2) from the combustion of fossil fuels has been identified as the major contributor to global warming and climate change. According to the Intergovernmental Panel on Climate Change (IPCC), this could lead to global warming of between 1.4 and 5.8 °C, more frequent severe weather conditions, and damage to many natural ecosystems.[1] To reduce these environmental concerns, there is considerable international collaboration to establish coal-based technologies that minimize CO_2 emission without significantly increasing costs. Separation and sequestration of CO_2 is a near-term goal for emission reduction.[2] Many ways can reduce CO_2 emissions, such as absorption, adsorption, and membrane separation. Although these processes have proved successful for the selective removal of CO_2 from multicomponent gaseous stream, they still have some critical problems associated with large energy consumption, corrosion, foaminess, and low capacity.[3−6] Recently, one promising technology, hydrate separation, has attracted more attention: Kang and Lee[7] proposed a hydrate-based crystallization process that can recover 99 mol % of CO_2 from flue gas.

Gas hydrates are crystalline composed of water and gas under suitable conditions of low temperature and high pressure. Fully loaded sI methane hydrate contains about 170 volumes of methane (STP) per volume of hydrate.[8] When gas hydrate is formed from a mixture of gases, the concentration of these gases in the hydrate phase and that in the gas phase is different. Consequently, the component that formed hydrate more easily might be enriched in hydrate phase. Due to hydrates having the capacity to store a large amount of gas and to separate a gas mixture, hydrate technology has attracted much attention as a potential means of capturing CO_2. The hydrate-based separation process was classified into two systems: (1) gas mixtures separation with hydrate, such as recovery CO_2 from flue gas[7] and separation H_2 from refinery,[9] and (2) solution separation with hydrate, such as desalination of seawater[10] and concentration of liquid foods by the use of gas hydrate.[11]

* To whom correspondence should be addressed. Telephone: +86-020-22236581. Fax: +86-020-22236581. E-mail: ssfan@scut.edu.cn.
† South China University of Technology.
‡ Dalian University of Technology.

(1) *IPCC, 2005: IPCC Special Report on Carbon Dioxide Capture and Storage. Prepared by Working Group III of the Intergovernmental Panel on Climate Change*; Metz, B., Davidson, O., de Coninck, H. C., Loos, M. L., Meyer, A., Eds.; Cambridge University Press: Cambridge and New York, 2005.
(2) Figueroa, J. D.; Fout, T.; Plasynski, S.; McIlvried, H.; Srivastava, R. D. *Int. J. Greenhouse Gas Control.* **2008**, *2*, 9–20.
(3) Douglas, A.; Costas, T. *Sep. Sci. Technol.* **2005**, *40*, 321–348.
(4) Yang, H.; Xu, Z.; Fan, M.; Gupta, R.; Slimane, R. B.; Bland, A. E.; Wright, I. *J. Environ. Sci.* **2008**, *20*, 14–27.
(5) Shaw, T. P.; Hughes, P. W. *Hydrocarbon Process.* **2001**, 53–58.
(6) Klara, S. M.; Srivastava, R. D. *Environ. Progress.* **2002**, *21*, 247–253.
(7) Kang, S. P.; Lee, H. *Environ. Sci. Technol.* **2000**, *34*, 4397–4400.
(8) Sloan, E. D.; Koh, C. A. *Clathrate Hydrates of Natural Gases*, 3rd ed.; CRC Press: Boca Raton, FL, 2008.
(9) Wang, X. L.; Chen, G. J.; Yang, L. Y.; Zhang, L. W. *Sci. China Ser. B.* **2008**, *51*, 171–178.
(10) Max, M. D. Hydrate Desalination or Water Purification. U.S. Patent 6,767,471B2, July 27, 2004.
(11) Purwanto, Y. A.; Oshita, S.; Seo, Y.; Kawagoe, Y. *J. Food Eng.* **2001**, *47*, 133–138.

10.1021/ef9003329 CCC: $40.75
Published on Web 07/13/2009

To reduce the energy consumption and accelerate the hydrate separation process, some additives have been used. Kang and Lee[7] developed a new hydrate-based gas separation process with THF. Addition of THF reduced the operating pressure and enhanced the corresponding kinetic rate. It was firmly verified that the hydrate-based gas separation process makes it possible to recover more than 99 mol % of CO_2 from flue gas by three hydrate separation stages. Seo et al.[12] studied CO_2-N_2 hydrate formation and hydrate phase equilibria for the ternary CO_2-N_2-water system in silica gel pores. It was possible to achieve concentrations of more than 96 mol % CO_2 gas in the product after three cycles of hydrate formation and dissociation. The kinetic studies with ^1H NMR microimaging showed that the dispersed water in the silica gel pore system reacted readily with the gas. Linga et al.[13,14] reported a medium-pressure CO_2 capture process based on hydrate crystallization in the presence of THF. The thermodynamic and kinetic data were utilized to develop the block flow diagram of the proposed process involving three hydrate stages coupled with a membrane-based gas separation process, which operated at 2.5 MPa and 273.75 K. Although these results are promising, the separation process with THF as an additive has some problems: for example, the temperatures required in the separation process are very low (0.6 °C); THF is harmful to health/safety and could contaminate environment, and the hydrate formation rate is still slow.

Recently, tetra-*n*-butyl ammonium salts have become an attractive environmentally friendly additive and achieved much attention, such as, TBAB and TBAF. TBAB or TBAF is a quaternary ammonium salt with a bromine or fluoride counterion commonly. They are used as phase transfer catalysts and mild base.There are many reports about the crystal structure and role of halogen anion in the semiclathrate hydrates.[15,16] Such a hydrate is called a semiclathrate hydrate crystal because a part of the cage structure is broken in order to encage the large tetra-*n*-butylammonium molecule, and it has been suggested that the semiclathrate hydrate crystal does not encage gas molecules.[17] Shimada et al.[17] first found that TBAB hydrate could encage methane molecules in mixtures of methane and propane or methane and ethane and deduced that these empty unsized cages of TBAB hydrate crystals function as a sieve for gas molecules. Then Kamata et al.[18] proposed that gases with small molecular size and high solubility in water can be effectively separated using TBAB semiclathrate hydrate. Duc et al.[19] studied CO_2 capture from a gas mixture by hydrate crystallization using TBAB as an additive and estimated investment and production cost by flowsheeting simulations. Most recently, Chapoy et al.[20] and Sakamoto et al.[21] also investigated the thermodynamic stability and hydrogen occupancy on the hydrogen−TBAF semiclathrate. They found that binary H_2-TBAF semiclathrate is more stable than H_2-TBAB semiclathrate.

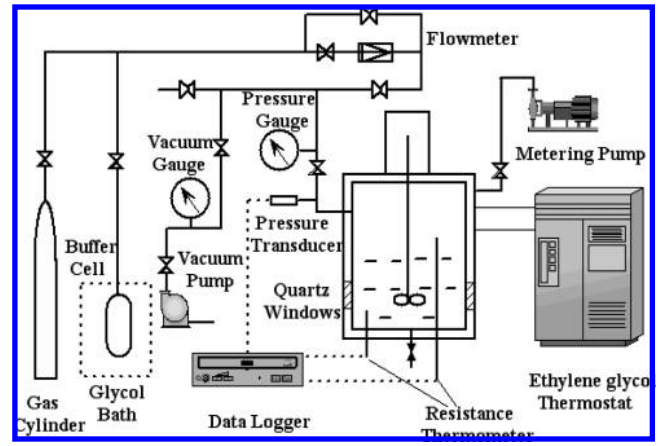

Figure 1. Schematic diagram of the experimental setup.

Even though TBAB has been proven as an effective additive for hydrate formation, however, the kinetic and separation efficiency of CO_2 capture by formation of semiclathrate hydrates have not been studied extensively, especially by forming TBAF semiclathrate hydrate.

In this paper, CO_2 capture from simulated flue gas (CO_2 (16.60 mol %)/N_2 binary mixtures) by formation of semiclathrate hydrates was investigated. The effect of TBAB and TBAF on hydrate formation kinetics under different conditions were studied; the space velocity of hydrate reactor, CO_2 recovery, and separation factor were calculated. Additionally, to obtain higher purity CO_2, we proposed a two-stage hydrate separation process with TBAF.

2. Experimental Section

2.1. Materials. The simulated flue gas containing CO_2(16.6 mol %)/N_2 and a gas mixture containing CO_2(53.5 mol %)/N_2 were supplied by Guangzhou Shengying Gas Co. Ltd. TBAB (99 wt % Guanghua Chemical Factory, China) and TBAF·$3H_2O$ (99 wt %, Shanghai HATCH Co. Ltd.) were weighed on an electronic balance with a readability of ±0.1 mg. Distilled water was used to prepare all solutions.

2.2. Apparatus. The schematic diagram of the experimental apparatus used is shown in Figure 1. It mainly consisted of a stainless-steel reactor (7.5 cm in diameter, effective volume 1 L) equipped with a magnetic stirrer (Hai'an Scientific Research Apparatus Co., China). The reactor was designed to be operated at pressures up to 20 MPa. Two quartz windows (4.5 cm in diameter) were mounted on both sides of the reactor. The temperature of the reactor was controlled by circulating the coolant from a thermostat (Huber CC1-K20B) with a stability of ±0.01 K inside the jacket around the cell. Two Pt100 resistance thermometers (Westzh WZ-PT100) within 0.1 K accuracy which are placed in the middle and bottom of the reactor, respectively, were used to monitor the temperature of the reactor. A pressure transducer (Westzh CyB-20S) within 0.01 MPa in accuracy measured the pressure inside of the reactor. The aqueous solution of TBAB or TBAF at a desired composition was introduced into the cell by a high-pressure metering pump (Alipu JX/12.5). The pressures and temperatures of the reactor were recorded by a data logger (Agilent 34970A). During the experiment the compositions of the gas phase were determined by gas chromatography (KeChuang GC9800: TCD detector, Porapak Q packed column).

2.3. Procedure. After 600 cm^3, 0.293 mol % TBAB or TBAF solution was introduced into the evacuated reactor, the reactor was cooled to the desired value. When the cell temperature was stabilized, the reactor was vacuumed and purged using a mixture gas of CO_2(16.60 mol %)/N_2 4−5 times to ensure the absence of

(12) Seo, Y. K.; Moudrakovski, I. L.; Ripmeester, J. A.; Lee, J. W.; Lee, H. *Environ. Sci. Technol.* **2005**, *39*, 2315–2319.
(13) Linga, P.; Kumar, R.; Englezos, P. *Chem. Eng. Sci.* **2007**, *62*, 4268–4276.
(14) Linga, P.; Adeyemo, A.; Englezos, P. *Environ. Sci. Technol.* **2007**, *42*, 315–320.
(15) Shimada, W.; Shiro, M.; Kondo, H.; Takeya, S.; Oyama, H.; Ebinuma, T.; Narita, H. *Acta Crystallogr., Sect. C* **2005**, *61*, o65–o66.
(16) Aladko, L. S.; Dyadin, Yu. A.; Rodionova, T. V.; Terekhova, I. S. *J. Mol. Liq.* **2003**, *106*, 229–238.
(17) Shimada, W.; Ebinuma, T.; Oyama, H.; Kamata, Y.; Takeya, S.; Uchida, T.; Nagao, J.; Narita, H. *Jpn. J. Appl. Phys.* **2003**, *42*, L129–L131.
(18) Kamata, Y.; Oyama, H.; Shimada, W.; Ebinuma, T.; Takeya, S.; Uchida, T.; Nagao, J.; Narita, H. *Jpn. J. Appl. Phys.* **2004**, *43*, 362–365.
(19) Duc, N. H.; Chauvy, F.; Herri, J. M. *Energy Convers. Manage.* **2007**, *48*, 1313–1322.
(20) Chapoy, A.; Anderson, R.; Tohidi, B. *J. Am. Chem. Soc.* **2007**, *129*, 746–747.
(21) Sakamoto, J.; Hashimoto, S.; Tsuda, T.; Sugahara, T.; Inoue, Y.; Ohgaki, K. *Chem. Eng. Sci.* **2008**, *63*, 5789–5794.

air, and then the mixture gas of CO_2/N_2 was charged into the cell until the given pressure. Then the stirrer was started to initiate hydrate formation (1100 rpm). During the experiment the temperature and pressure were recorded. After hydrate formation finished (the system pressure was stable), the stirrer was stopped and the residual gas was transferred and analyzed with GC. Then the vent valve was opened, the remaining gas was purged, and the vessel was warmed to 25 °C to make the hydrate dissociate completely. The dissociated gas composition was also determined with GC.

3. Calculation of the Hydrate Formation Rate and Separation Efficiency

3.1. Hydrate Formation Rate Constant. The hydrate formation rate can be expressed in terms of fugacity difference during formation and at equilibrium.[22,23] In this study, the chemical potential difference was used as the driving force and the apparent gas uptake rate ($-dn/dt$) is expressed as

$$\left(-\frac{dn}{dt}\right) = aK^*(\mu_g - \mu_{eq}) \tag{1}$$

$$\frac{1}{K^*} = \frac{1}{k_f} - \frac{1}{k_L} \tag{2}$$

where a is the interfacial area, K^* is the overall kinetic constant, μ_g and μ_{eq} are chemical potentials of the guest molecule in the gas phase and in the hydrate phase, respectively, k_f is the crystal growth constant, and k_L is the mass transfer coefficient in the liquid phase.

Under the conditions of this study, $1/k_L$ could be eliminated by a vigorous stirring (1100 rpm) in the reactor ($1/k_f \gg 1/k_L$). Thus, the hydrate rate can be expressed by

$$r_f = \left(-\frac{dn}{dt}\right) = ak_f(\mu_g - \mu_{eq}) = ak_f RT \ln\frac{f_g}{f_{eq}} \tag{3}$$

$$r_f = \left(\frac{\Delta n}{\Delta t}\right) = \frac{V_g}{RT}\frac{(f_g - f_{eq})}{\Delta t} \tag{4}$$

where f_g and f_{eq} are the fugacity of the gas phase and the hydrate phase at equilibrium conditions, respectively, calculated by the SRK equation of state, V_g is the volume of the gas phase, and Δt is the time to reach equilibrium for the hydrate separation process. Due to it being difficult to separate the term a and k_f from the experimental results for the fugacity change, the hydrate rate constant is expressed as

$$ak_f = \frac{V_g}{(RT)^2}\frac{(f_g - f_{eq})}{\Delta t \ln(f_g/f_{eq})} \tag{5}$$

3.2. Molar Number of Gas Consumed. The molar number of gas that has been consumed during hydrate formation can be calculated as follows

$$\Delta n = n_z - n_{eq} = \frac{P_z V_g}{z_z RT} - \frac{P_{eq} V_g}{z_{eq} RT} \tag{6}$$

where z is the compressibility factor calculated by the PR equation of state and subscripts z and eq refer to the component of the feed gas mixture and equilibrium gas mixture. The volume of gas was assumed constant throughout the hydrate formation process (volume changes due to the phase transitions were neglected).

3.3. Space Velocity of Hydrate Reactor. The space velocity (SV), in chemical reactor design, indicates how many reactor volumes of feed that can be treated per time unit and is defined as[24]

$$SV \equiv \frac{v_0}{V_R} \tag{7}$$

where v_0 is the gas volumetric flow rate and V_R is the volume of the reactor. The space velocity commonly used in industry for reactions involving gas consumption is gas hourly space velocity (GHSV), in which the gas volumetric flow rate, v_0, is normally measured at standard temperature and pressure (STP).

$$GHSV = \frac{v_0(STP)}{V_R} \tag{8}$$

Thus, in this batch hydrate separation experiment v_0 could be defined as[25]

$$v_0 = \frac{\Delta n V_m(STP)}{\Delta t} \tag{9}$$

where Δn is the gas moles that has been consumed during hydrate formation, V_m is the mole volume of the hydrate forming gas mixture at standard temperature and pressure (STP), and Δt is the time to reach equilibrium for the hydrate separation process. Thus, the GHSV can be expressed by

$$GHSV = \frac{\Delta n V_m(STP)}{V_R \Delta t} \tag{10}$$

3.4. CO_2 Recovery and Separation Factor. The CO_2 recovery of mixed gas in the hydrate phase is calculated as follows[14]

$$R = \frac{n_{x,1}}{n_{z,1}} \tag{11}$$

where $n_{z,1}$ is defined as the molar number of CO_2 in the feed gas and $n_{x,1}$ is the molar number of CO_2 in the hydrate phase at the end of the experiment. The separation factor is calculated as follows

$$S = \frac{x_1/y_1}{x_2/y_2} \tag{12}$$

where x_1 and y_1 are the concentration of CO_2 in the hydrate phase and gas phase at the end of the experiment, respectively. x_2 and y_2 are the concentration of N_2 in the hydrate phase and gas phase at the end of the experiment, respectively.

4. Results and Discussion

4.1. Hydrate Formation Kinetics. *4.1.1. Hydrate Formation Process.* The typical trends of the feed pressure during the hydrate formation process in the presence of 0.293 mol % TBAB and TBAF at 4.5 °C for CO_2(16.6 mol %)/N_2 binary mixture gas are shown in Figures 2 and 3, respectively. The results

(22) Englezos, P.; Kalogerakis; Dholabhaiand, P. D.; Bishnoi, P. R. *Chem. Eng. Sci.* **1987**, *42*, 2647–2658.

(23) Daimaru, T.; Yamasaki, A.; Yanagisawa, Y. *J. Pet. Sci. Eng.* **2007**, *56*, 89–96.

(24) Fogler, H. S. *Elements of Chemical Reaction Engineering*, 3rd ed.; Prentice Hall: New York, 1999.

(25) Mori, Y. H. *J. Chem. Ind. Eng. (China)* **2003**, *54*, 1–17.

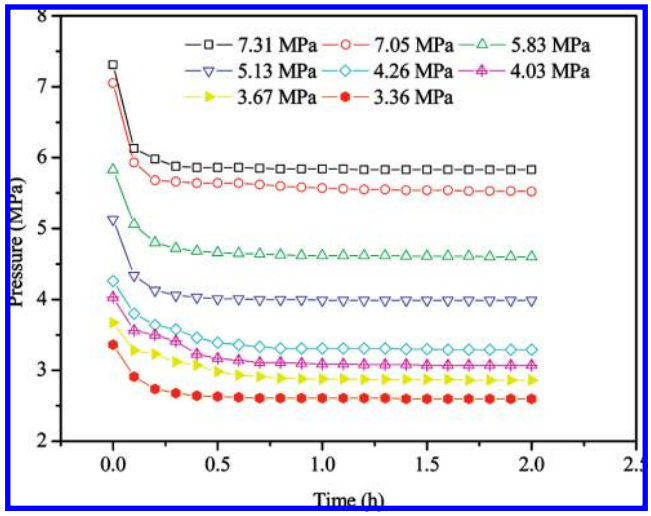

Figure 2. Pressure as a function of time during experiment at 4.5 °C and 0.293 mol % TBAB from 3.36 to 7.31 MPa.

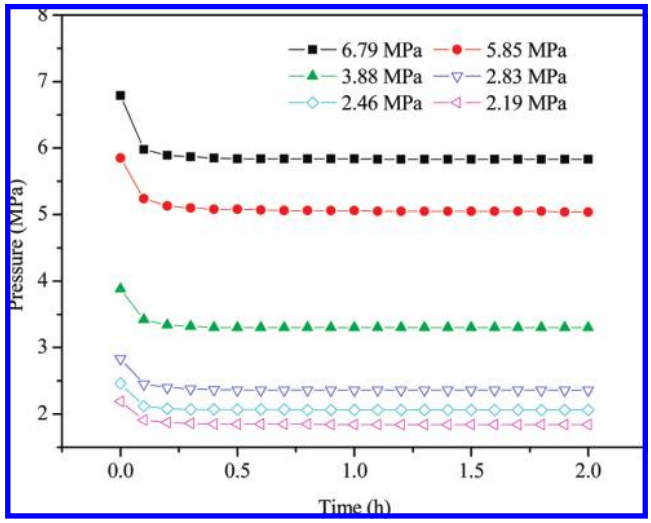

Figure 3. Pressure as a function of time during experiment at 4.5 °C and 0.293 mol % TBAF from 2.19 to 6.79 MPa.

revealed the system pressure decreased rapidly during the first 0.5 and 0.25 h and then were stable, which indicated that hydrate formation had completed and the system reached equilibrium. Figures 2 and 3 show a comparison of the effect of TBAB and TBAF on gas mixture hydrate formation. It took 0.5−1 h for the system pressure to reach equilibrium with TBAB, while it took only about 0.25 h with TBAF. Compared to the times with the data of reference,[14] it was found that the time of hydrate equilibrium with TBAF is about one-half of that with TBAB and one-fourth of that with THF. It was worth noticing that hydrate can form even under the lower feed pressure with TBAF, such as 2.19 MPa at 4.5 °C. These results demonstrated that the acceleration effect of TBAF was better than TBAB and THF. The pressure drops against feed pressure with TBAB and TBAF, which is shown in Figure 4. The pressure drops varied from 0.76 to 1.59 MPa with TBAB and from 0.35 to 0.96 MPa with TBAF. Under the same feed pressure, the pressure drop of TBAB was more severe than that of TBAF. Meanwhile, for both of them the pressure drops increased with the enhancement of feed pressure, indicating that more CO_2/N_2 mixed gas was encaged in semiclathrate hydrate in the presence of TBAB. Even though larger drop pressures were obtained with TBAB, it did not mean that the CO_2 separation efficiency with TBAB is better than TBAF. The CO_2 separation efficiency is

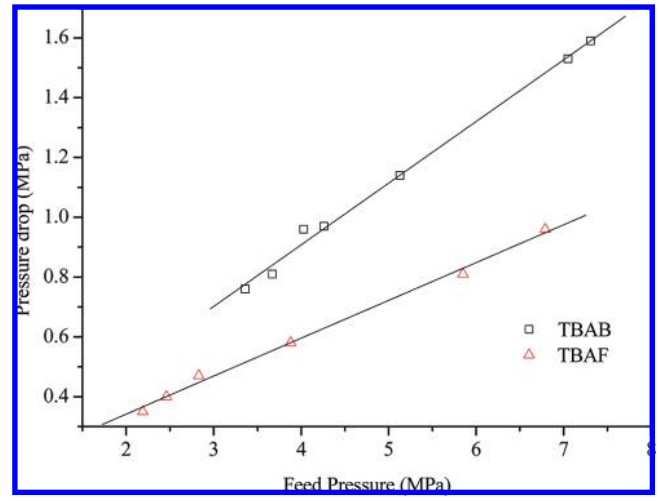

Figure 4. Relation between the pressure drop and feed pressure in the presence of TBAB and TBAF.

Table 1. Comparison of the Hydrate Formation Rate Constant with TBAB and TBAF at 4.5 °C

additive	feed pressure (MPa)	ak_f (mol^2/(s•J)) × 10^{-7}
TBAB	3.36	0.59
	3.67	0.72
	4.03	0.88
	4.26	0.99
	5.13	1.70
	7.05	2.46
	7.31	2.82
TBAF	2.19	1.38
	2.46	1.85
	2.83	2.12
	3.88	3.60
	5.85	5.41
	6.79	8.26

also determined by the concentration of CO_2 in the hydrate phase. A larger pressure drop with TBAB could be interpreted by the differences of the structure of TBAB and TBAF. In TBAB hydrate only 5^{12} small cages could encage gas molecules, which could not selectively encage CO_2 or N_2 by the ratio of molecular diameters to cavity diameters.[18] Thus, more N_2 could be encaged in 5^{12} small cages, which caused a large pressure drop in the vapor phase and high N_2 concentration in the hydrate phase. However, in TBAF, many $5^{12}6^2$ large cages could encage much larger molecular-CO_2 and little N_2 was encaged in TBAF hydrate. The deduction could be confirmed by the data of the composition of the vapor and hydrate phases.

4.1.2. Hydrate Formation Rate Constant. The hydrate formation rate constant calculated by eq 5 in the presence of TBAB and TBAF is displayed in Table 1. The results showed that the hydrate formation constants were one order of magnitude higher than the results of CH_4 hydrate,[23] which were in the presence of different surfactants. It revealed that the hydrate formation rate constant increased with increasing feed pressure. It was because the higher the feed pressure, the larger the driving force obtained, and it was consistent with the trends of the feed pressure during hydrate formation. Additionally, when the feed pressure of TBAB and TBAF was the same, the hydrate formation rate constant with TBAF was much faster than that with TBAB, for example, as the feed pressures were about 3.70 MPa, the hydrate formation rate constants with TBAB and TBAF were 0.72×10^{-7} and 3.60×10^{-7} mol^2/(s•J), respectively.

4.1.3. Space Velocity of Hydrate Reactor. It is generally difficult to compare the hydrate formation rate data from different sources on a common basis. Mori[25] first proposed the

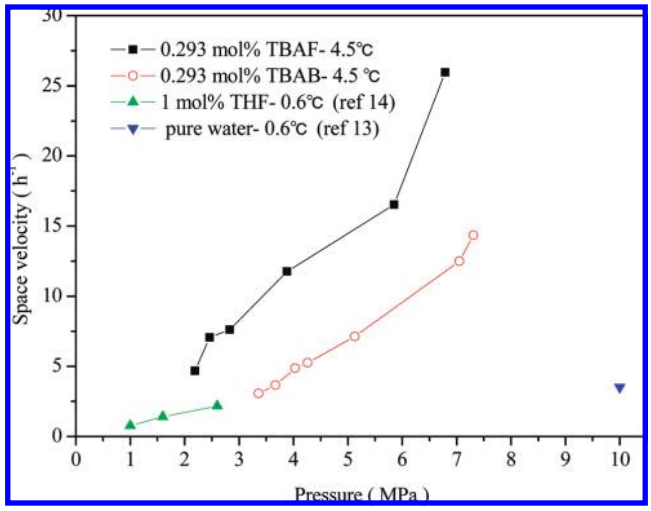

Figure 5. Space velocity as a function of feed pressure in different conditions.

Table 2. Vapor and Hydrate Equilibria Composition for the $CO_2(1)/N_2(2)-TBAB-H_2O$ System (where the TBAB concentration is 0.293 mol %)

T (°C)	P (MPa)	z_1 (%)	x_1 (%)	y_1 (%)	K_1
4.5	3.36	16.60	32.22	5.02	0.16
	3.67		35.62	5.52	0.15
	4.03		36.53	5.63	0.15
	4.26		29.43	5.76	0.20
	5.13		26.43	6.36	0.24
	7.05		23.52	6.80	0.20
	7.31		22.57	7.09	0.24

definition of the normalized rate of guest-gas supply to compare the data of different literature reports. In this paper, we proposed the space velocity to compare the capacity of the hydrate separation processing, which is commonly used in reaction engineering. Figure 5 shows the space velocity of the hydrate reactor calculated using eq 10 as a function of pressure in the presence of TBAB and the space velocity calculated using the data of refs 13 and 14. The space velocity increased with increasing feed pressure in the presence of TBAB, TBAF, and THF, and the space velocity of the hydrate separation process with TBAB and TBAF was much more than that with THF. The hydrate formation pressure was reduced with 1 mol % THF, but the space velocity dropped from 3.51 h^{-1} without additive to 0.77 h^{-1}. The space velocity reached a maximum of 25.96 with TBAF and 13.46 with TBAB. In Figure 5, when the feed pressure was more than 5.85 MPa in the presence of TBAF, the slope of the curve of the space velocity changed significantly with the feed pressure. The same result was also observed in the presence of TBAB with a feed pressure larger than 7.05 MPa. It implied that the space velocity increased remarkably due to much more gas mixture being encaged in the hydrate phase.

4.2. Composition of the Vapor and Hydrate Phases. The vapor and hydrate equilibria composition in the presence of TBAB and TBAF at 4.5 °C are shown in Tables 2 and 3. The influence of the feed gas pressure was investigated when the CO_2 content in the feed gas was 16.60 mol %. It should be noted that the compositions of the vapor phase and hydrate phase in this work are both in water and TBAB/TBAF-free basis. z_1, x_1, and y_1 represent the concentration of CO_2 in the feed gas, hydrate phase, and vapor phase, respectively. K_1 is the partition coefficient of CO_2 between the vapor and hydrate phase, $K_1 = y_1/x_1$.[26]

Table 3. Vapor and Hydrate Equilibria Composition for the $CO_2(1)/N_2(2)-TBAF-H_2O$ System (where the TBAF concentration is 0.293 mol %)

T (°C)	P (MPa)	z_1 (%)	x_1 (%)	y_1 (%)	K_1
4.5	2.19	16.60	51.72	3.20	0.062
	2.46		56.55	3.40	0.060
	2.83		49.86	3.75	0.075
	3.88		45.92	4.02	0.088
	5.85		40.09	4.52	0.11
	6.79		40.02	5.42	0.12

Table 4. Vapor and Hydrate Equilibria Composition for the $CO_2(1)/N_2(2)-TBAF-H_2O$ System (where the temperature and TBAF concentration are 7.1 °C and 0.293 mol %, respectively)

T (°C)	P (MPa)	z_1 (%)	x_1 (%)	y_1 (%)	K_1
7.1	2.39	16.60	47.11	3.83	0.080
	3.33		47.26	3.20	0.068
	4.11		54.53	3.59	0.066
	4.39		46.84	3.65	0.078
	6.45		35.36	4.30	0.12

In Table 2, the CO_2 concentration in the hydrate phase changed from 22.57 to 36.53 mol % with the feed pressure varying from 3.36 to 7.31 MPa, and it showed a maximum at 4.03 MPa. The result demonstrated that CO_2 could be enriched in the hydrate phase in the presence of TBAB. Comparing the data in Table 2, CO_2 can enrich in the hydrate phase remarkably even under lower feed pressure, which also can be drawn from the K_1 value. CO_2 concentrations in the hydrate phase were higher than 40.09 mol %, particularly in the presence of TBAF; it reached a maximum of 56.55 mol %. It was attributed to the structure of TBAF semiclathrate hydrate. Shimada et al.[15] and Davidson[27] proposed the hydrate structure of $TBAB \cdot 38H_2O$ and $TBAF \cdot 32H_2O$ as $6(5^{12})4(5^{12}6^2)4(5^{12}6^3) \cdot 76H_2O$ and $10(5^{12})4[3(5^{12}6^2)1(5^{12}6^3)]4(5^{12}6^2) \cdot 172H_2O$, respectively. It was clear that there are more ($5^{12}6^2$) cages in the TBAF semiclathrate hydrate than in TBAB's, which can encage CO_2 easily. Consequently, the CO_2 concentration in the TBAF semiclathrate hydrate phase could be higher than in the TBAB semiclathrate hydrate. The structures of $TBAB \cdot 38H_2O$ and $TBAF \cdot 32H_2O$ also revealed the reason why larger pressure drops were obtained with TBAB, but the CO_2 concentrations in the hydrate phase were lower than those with TBAF. CO_2 and N_2 molecules competed with each other to occupy 5^{12} small cages in TBAB hydrate.

To verify the effect of temperature on the CO_2 concentration in the hydrate phase, the hydrate formation process was studied at 7.1 °C. As seen in Tables 3 and 4, under the same feed pressure, the CO_2 concentration in the hydrate phase decreased with increasing system temperature. As the concentration of CO_2 in the hydrate phase reached the maximum, the corresponding feed pressure increased with increasing system temperature. Thus, it could be concluded that a low temperature was beneficial to encage CO_2 in TBAF semiclathrate hydrate.

4.3. CO_2 Recovery. As shown in Figure 6, the CO_2 recovery calculated using eq 11 with TBAB changed from 35.8 to 53.0 mol % in the feed pressure range from 3.36 to 7.31 MPa at 4.5 °C. CO_2 recovery in the presence of TBAF changed from 33.9 to 56.0% in the feed pressure range from 2.19 to 6.79 MPa at 4.5 °C. CO_2 recovery (about 50%) was similar to the results of ref 14 in the presence of THF and ref 13 with pure water. It

(26) Wilcox, W. I.; Carson, D. B.; Katz, D. L. *Ind. Eng. Chem.* **1941**, *33*, 662–665.

(27) Davidson, D. W. In *Water: A Comprehensive Treatise*; Franks, F., Eds.; Plenum Press, New York, London, 1973; Vol. 2, Chapter 3, pp 115–234.

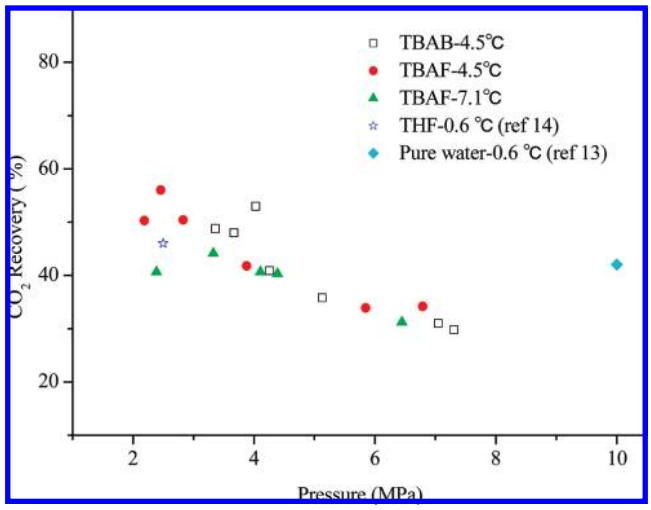

Figure 6. Relation between the CO_2 recovery and feed pressure in the presence of TBAB and TBAF.

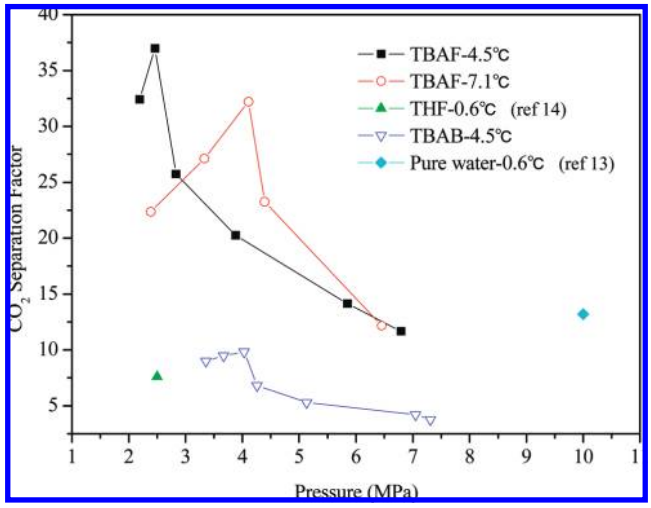

Figure 7. Relation between the CO_2 separation factor and feed pressure in the presence of TBAB and TBAF.

Table 5. Vapor and Hydrate Equilibria Composition for the CO_2(1)/N_2(2)−TBAF−H_2O System (where the feed concentration of CO_2 is 53.50 mol %)

T (°C)	P (MPa)	z_1 (%)	x_1 (%)	y_1 (%)	iK$_1$
4.5	0.74	53.50	83.28	34.45	0.41
	0.90		90.40	30.61	0.34
	1.23		88.41	31.65	0.36
	1.51		85.06	32.72	0.38
	2.23		84.37	33.93	0.40

was also concluded that the effect of the feed pressure on CO_2 recovery was small. The results showed that the same amount of CO_2 in the feed gas mixture was encaged in the hydrate phase in different pressures, but the trend of N_2 encaged in hydrate could increase at higher feed pressure.

4.4. Separation Factor. Figure 7 displays the CO_2 separation factor calculated using eq 12 at different conditions and the results of refs 13 and 14. The CO_2 separation factors with TBAF were much higher than those with TBAB and THF under the same feed pressure. For example, at 4.5 °C, the optimum CO_2 separation factor with TBAF was 36.98; however, it was only 9.82 with TBAB. It was also found that the enhancement of the feed pressure was a disadvantage to CO_2 separation, which is due to the fact that N_2 can easily compete with CO_2 for cage occupancy with higher driving force.

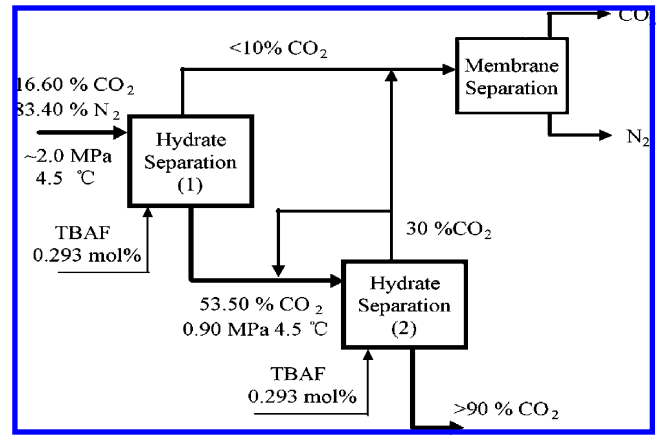

Figure 8. Two-stage hybrid hydrate−membrane separation process for CO_2 recovery from a CO_2(16.60 mol %)/N_2 mixture in the presence of TBAF.

As mentioned in the previous sections, TBAF was better than TBAB for capturing CO_2 by forming hydrate. To obtain higher purity CO_2, a second stage CO_2/N_2 separation process with TBAF in which the composition of the feed mixture gas was the composition of the hydrate phase of the first stage separation process was performed. As Table 5 shows, when the CO_2 concentration was 53.50 mol % in the feed mixture gas, CO_2 could be enriched to a maximum concentration of 90.40 mol % with a feed pressure of 0.90 MPa.

5. Two-Stage Hydrate Separation Process

On the basis of the above results, a conceptual flow sheet for capture of CO_2 from the CO_2/N_2 mixture is presented in Figure 8. A two-stage hydrate separation process combined with membrane separation was designed. The feed pressures of the two stages were 2.00 and 0.90 MPa, respectively. Thus, it was possible that a 90 mol % CO_2 stream can be obtained from a CO_2(16.60 mol %)/N_2 mixture under gentle pressure by only a two-stage hydrate separation process.

6. Conclusions

The effect of TBAB and TBAF on the hydrate formation rate and separation efficiency were investigated during capture of CO_2 from simulated flue gas (CO_2(16.60 mol %)/N_2 binary mixtures) by formation of semiclathrate hydrates. The following conclusions can be drawn.

(1) TBAB and TBAF could accelerate hydrate formation and reduce the corresponding feed pressure at the same temperature. Moreover, the time to reach hydrate equilibrium with TBAF was about one-half of that with TBAB and one-fourth of that with THF.

(2) Under the same feed pressure, the hydrate formation rate constant with TBAF was much higher than that with TBAB. In addition, the hydrate formation rate constant increased with increasing feed pressure and reached the maximum at 2.82×10^{-7} mol^2/(s·J) with TBAB and 8.26×10^{-7} mol^2/(s·J) with TBAF.

(3) The space velocity of the hydrate reactor increased with increasing feed pressure and reached a maximum of 25.96 h^{-1} with TBAF and 13.46 h^{-1} with TBAB, which was much more than that with THF.

(4) With the existence of TBAB and TBAF, CO_2 was enriched in the hydrate phase, and the maximum CO_2 concentration in the hydrate phase was 36.52 mol % with TBAB at 4.03 MPa and 56.55 mol % with TBAF at 3.67 MPa. CO_2

recovery was about 50%, and the optimum CO_2 separation factor with TBAF (36.98) was much higher than those with TBAB and THF. The higher feed pressure was a disadvantage to improving the CO_2 separation factor with TBAB or TBAF.

(5) CO_2 could be enriched to 90.40 mol % from CO_2(16.60 mol %)/N_2 binary mixtures under the low feed pressure by two stages of hydrate separation with TBAF.

Acknowledgment. The authors greatly acknowledge the National Natural Science Foundation of China (No. 20876019) and the National High Technology Research and Development Program ("863" Program) of China (No. 2007AA03Z229).

Nomenclature

$-(dn)/(dt)$ = apparent gas uptake rate (mol/s)
a = interfacial area (m^2)
K^* = overall kinetic constant ($mol^2/(m^2 \cdot s \cdot J)$)
μ = chemical potential
k_f = crystal growth constant ($mol^2/(m^2 \cdot s \cdot J)$)
k_L = mass transfer coefficient in the liquid phase ($mol^2/(m^2 \cdot s \cdot J)$)
f = fugacity (MPa)
V = volume (m^3)
ak_f = hydrate rate constant ($mol^2/(s \cdot J)$)
r_f = hydrate rate (mol/s)
Δn = molar number of gas consumed (mol)
Δt = time to reach equilibrium for hydrate separation (s)
n = molar number of gas (mol)
P = pressure (MPa)
z = compressibility factor
R = universal gas constant ($J \cdot mol^{-1} \cdot K^{-1}$)
T = temperature (K)
SV = space velocity (h^{-1})
v_0 = gas volumetric flow rate ($m^3 \cdot h^{-1}$)
GHSV = gas hourly space velocity (h^{-1})
V_m = mole volume of hydrate forming gas mixture at standard temperature and pressure (STP) (m^3/mol)
R = CO_2 recovery
S = CO_2 separation factor
K = partition coefficient of CO_2 between the vapor and hydrate phase
x = concentration of equilibrium vapor phase (mol %)
y = concentration of hydrate phase (mol %)
z = concentration of feed gas phase (mol %)

Subscripts

g = gas phase
R = reactor
z = feed gas
eq = hydrate equilibrium
x = equilibrium gas phase
1 = CO_2
2 = N_2

EF9003329